Available online at www.sciencedirect.com
ScienceDirect
International Journal of Heat and Mass Transfer 50 (2007) 4297–4310
International Journal of HEAT and MASS TRANSFER
www.elsevier.com/locate/ijhmt

Unstable and stable flow boiling in parallel microchannels and in a single microchannel

Guodong Wang, Ping Cheng *, Huiying Wu

School of Mechanical and Power Engineering, Shanghai Jiaotong University, 800 Dong Chuan Road, Shanghai 200240, PR China

Received 29 November 2006; received in revised form 26 January 2007
Available online 29 May 2007

Abstract

A simultaneous visualization and measurement study have been carried out to investigate flow boiling instabilities of water in microchannels at various heat fluxes and mass fluxes. Two separate flow boiling experiments were conducted in eight parallel silicon microchannels (with flow interaction from neighboring channels at headers) and in a single microchannel (without flow interaction), respectively. These microchannels, at a length of 30 mm, had an identical trapezoidal cross-section with a hydraulic diameter of 186 μm. At a given heat flux and inlet water temperature, it was found that stable and unstable flow boiling regimes existed, depending on the mass flux. A flow boiling map, in terms of heat flux vs mass flux, showing stable flow boiling regime and unstable flow boiling regime is presented for parallel microchannels as well as for a single microchannel, respectively, at an inlet water temperature of 35 °C. In the stable flow boiling regime, isolated bubbles were generated and were pushed away by the incoming subcooled liquid. Two unstable flow boiling regimes, with long-period oscillation (more than 1 s) and short-period oscillation (less than 0.1 s) in temperature and pressure, were identified. The former was due to the expansion of vapor bubble from downstream while the latter was owing to the flow pattern transition from annular to mist flow. A comparison of results of flow boiling in parallel microchannels and in a single microchannel shows that flow interaction effects from neighboring channels at the headers are significant.

Keywords: Boiling instability; Heat transfer; Microchannels; Instability; Reversed flow

1. Introduction

It is well known that two-phase flow instabilities in a macrochannel can be divided into dynamic and static categories depending on the mechanism [1,2]. The dynamic instability generally reflects the feed back control process of a number of parameters such as pressure, mass flux, and temperature. It is commonly recognized that three types of oscillations exist in a macrochannel: pressure drop oscillation, density wave oscillation and thermal oscillation [3,4]. These unsteady behaviors can introduce a boiling crisis that causes mechanical damages [5]. As pointed out by Boure et al. [1], pressure wave oscillations had been observed in subcooled boiling, bulk boiling, and film boiling under subcritical or supercritical conditions [6]. Several investigators have reported pressure oscillations of relatively high frequency in the range of 10–100 Hz (0.01–0.1 s), when operating under highly subcooled conditions.

Recently, a great deal of attention has been given to the study of dynamic flow boiling instability in microchannels [8–17]. In particular, Hetsroni et al. [8,9] found small pressure fluctuations in their investigation of flow boiling of water in 21 silicon triangular microchannels having a diameter of 129 μm, and observed periodic annular flow and the periodic dry steam flow in these microchannels. Brutin et al. [10] investigated heat and mass transfer and analyzed two-phase flow instabilities in vertical rectangular microchannels with a hydraulic diameter of 889 μm. It was found that steady and unsteady thermo-hydraulic behaviors depended on the amount of heat flux and mass flux. Qu and Mudawar [11] performed a flow boiling experiment

* Corresponding author. Tel.: +86 21 6293 3107; fax: +86 21 6293 3107.
E-mail address: pingcheng@sjtu.edu.cn (P. Cheng).

0017-9310/$ - see front matter © 2007 Elsevier Ltd. All rights reserved.
doi:10.1016/j.ijheatmasstransfer.2007.01.033

Nomenclature

A_c	cross-sectional area of microchannel	t	time
A_w	area of heating area	T	Temperature
h_{fg}	latent heat of evaporation		
G	mass flux	*Greek symbol*	
M	total mass	Φ	heat transfer ratio
N	total number of microchannels		
q	heat flux	*Subscripts*	
I	electric current of heater	in	inlet
V	electric voltage of heater	out	outlet
P	pressure	w	wall

of water in a two-phase microchannels heat sink made of 21 copper parallel microchannels with a cross-section area of $231 \times 713\ \mu m^2$. They identified two types of two-phase hydrodynamic instabilities in the microchannels: severe pressure drop oscillation and mild parallel channel instability. Wu and Cheng [12,13] carried out a simultaneous visualization and measurement investigation on flow boiling of water in parallel silicon microchannels of trapezoidal cross-section having hydraulic diameters of 82.8 μm, 158.8 μm, and 185.6 μm, respectively. They found for the first time that there existed two oscillatory flow boiling modes with large amplitudes of temperature and pressure fluctuations in microchannels: liquid/two-phase alternating flow (LTAF) and liquid/two-phase/vapor alternating flow (LTVAF). They also found that the oscillations of mass flux and pressure drop were out of phase in these two boiling modes. Subsequently, Xu et al. [14] conducted experiments to study dynamic flow instability of methanol in a compact heat sink consisting of 26 rectangular microchannels with 300 μm width and 800 μm depth. Their study showed that once the mass flux became smaller than that of onset of flow instability, three types of oscillations occurred: large amplitude/long-period oscillation, small amplitude/short-period oscillation, and thermal oscillation. Steinke and Kandlikar [15] performed an experimental investigation for flow boiling using water in six parallel horizontal microchannels with a hydraulic diameter of 207 μm. The flow visualization demonstrated that the flow reversal condition in parallel flow channels was due to bubble nucleation followed by its rapid growth. In addition, the dry-out condition was observed. Most recently, Hetsroni et al. [16] observed the explosive boiling phenomena with periodic wetting and dry-out in triangular silicon microchannels, and found that the trigger mechanism of such a phenomenon was the venting of elongated bubble due to very rapid expansion.

In this paper, we have performed further simultaneous visualization and measurement study to investigate dynamic instabilities in flow boiling of water in parallel microchannels as well as in a single microchannel, having a hydraulic diameter of 186 μm that were used in our previous studies [12,13]. It was found that after incipient boiling, both stable and unstable flow boiling occurred in the parallel microchannels and a single microchannel depending on the heat-to-mass flux ratio, q/G. Unstable flow boiling with long-period oscillation (more than 1 s) and short-period oscillation (less than 0.1 s) existed due to different flow patterns. These instabilities due to the transition of flow patterns are called dynamic instabilities according to Boure et al. [1]. Periods and amplitudes of temperatures, pressures, and mass flux fluctuations in these dynamic instabilities were measured. With the aid of a microscope and a high-speed video recording system, flow boiling patterns at various heat flux and mass flux conditions were observed. In addition, a map, in terms of heat flux versus mass flux, showing stable and unstable flow boiling regimes in parallel microchannels as well as in a single microchannel is presented separately for an inlet water temperature of 35 °C.

2. Description of the experiment

2.1. Experimental setup

Fig. 1 shows the experimental setup, which consisted of a high-pressure tank, three valve regulators, a degassing unit, a constant temperature bath, a filter, a test section, and a collecting container. The deionized and degassed water in the pressure tank, being pushed by the compressed nitrogen gas, flowed successively through a ball valve, a degassing unit which removed the dissolved nitrogen gas, a constant temperature bath with the function of insuring a certain inlet water temperature, a needle valve to regulate the mass flux, a filter, to the test section heated by a film heater, and finally was collected in a container with a small hole vented to the atmosphere. The container was placed on a precision electronic balance, and the average mass flux of water was determined by calculating the mass increment per unit time.

2.2. Test section and measurement system

Fig. 2a shows the geometry and dimensions of the eight parallel microchannels having the same trapezoidal cross-

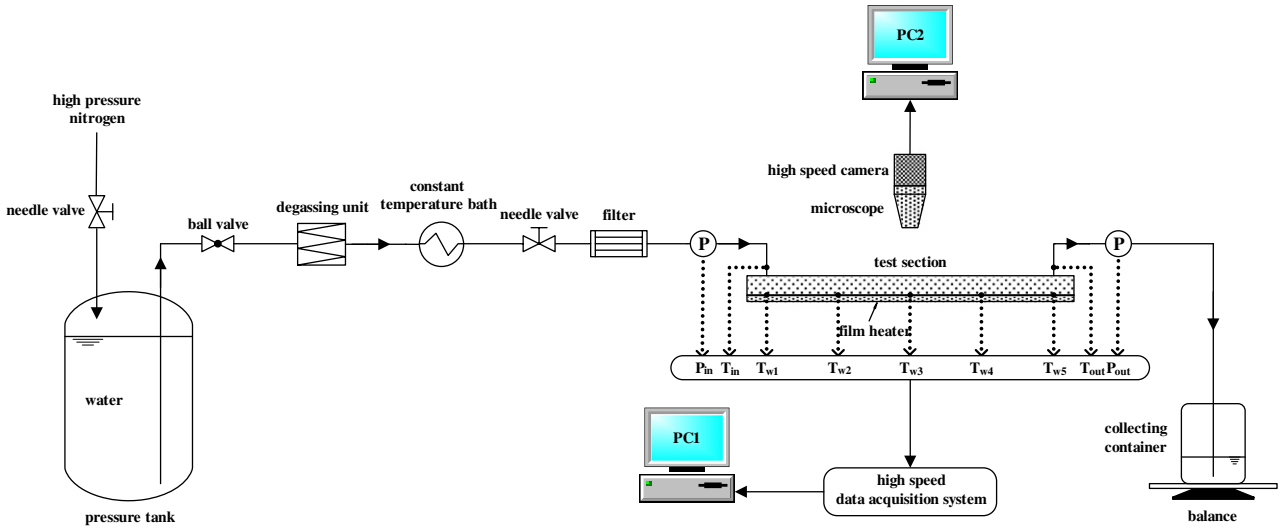

Fig. 1. Experimental test loop.

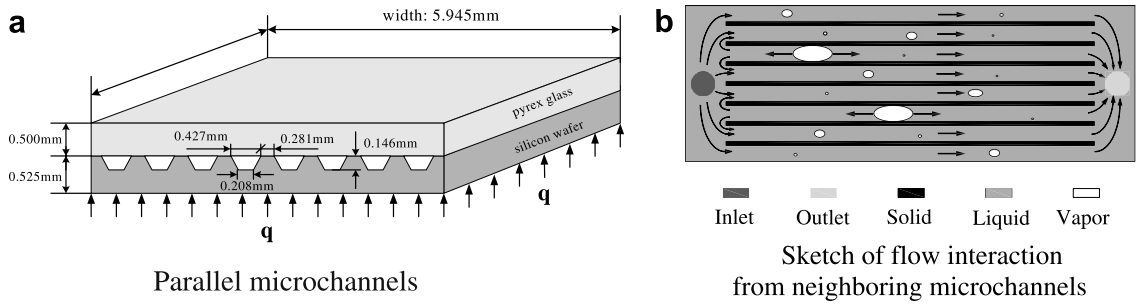

Fig. 2. Arrangement and flow interaction of parallel microchannels.

sectional area on a silicon substrate. The top width, bottom width, and depth of these trapezoidal microchannels were 427 μm, 208 μm, and 146 μm, respectively. These microchannels, having a hydraulic diameter of 186 μm and a length of 30 mm, were the same as in our previous work [12,13]. The distance between two neighboring microchannels was 281 μm. Fig. 2b shows a schematic representation of flow interaction from neighboring channels at the headers, where the unsynchronical expansion of vapor bubbles in neighboring parallel microchannels led to flow interaction at the headers. The geometry and dimensions of a single microchannel were exactly the same as parallel microchannels except the number of channel. The microchannels, etched in a ⟨1 0 0⟩ silicon wafer, were sealed from the top by a thin pyrex glass plate which allowed visualization of the boiling phenomena occurring inside the microchannels. A microscope and a high-speed video recording system, located above the microchannels, were used for the visualization study.

The test section was discussed in details in our previous work [12,13] and therefore, will not be repeated here. As shown in Fig. 3, T_{w1}, T_{w2}, T_{w3}, T_{w4}, and T_{w5} were the wall temperatures, T_{in} and T_{out} were temperatures of the fluid in the inlet plenum and outlet plenum. These temperatures were measured by seven type-T thermocouples, having a diameter of 0.1 mm with a response time of 0.1 s. Two pressure transducers with a response time of 0.001 s were used to measure water pressure (P_{in} and P_{out}) at the inlet and outlet of the microchannels.

The heat flux, q, was computed from $q = \Phi VI/A_w$, where V and I are the input voltage and current to the film heater, A_w the area of heated wall, and Φ the ratio of the heat absorbed by the working fluid to the total power input to the film heater. A set of single-phase heat transfer experiments were performed before the boiling heat transfer tests started. The range of the heat transfer ratio, Φ, ranging from 0.82 to 0.94 was determined. Thus, the mean heat transfer ratio of 0.88 was used to compute the effective heating power. The method was similar to that used by Xu et al. [7] and Hetsroni et al. [8], which was also used in our previous work [12,13]. The average mass flux of water was given by $G = \Delta M/(\Delta t \cdot N \cdot A_c)$, where ΔM is the total mass increment in the container measured by the electronic balance during an appropriate time interval Δt; N is the total number of microchannels and A_c is the cross-sectional area of the microchannel. Thus, the mass flux reported in this paper, is an average mass flux during Δt and is therefore not an instantaneous value.

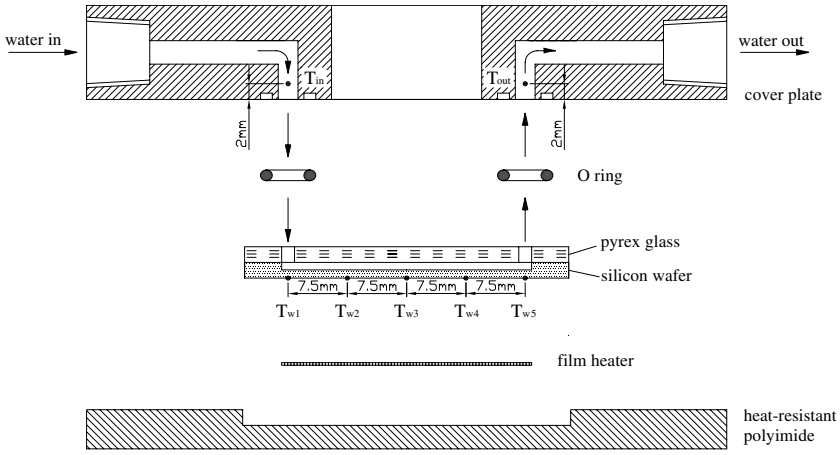

Fig. 3. Test section construction.

3. Results and discussion

3.1. Flow boiling patterns in parallel microchannels

Experiments for parallel microchannels were carried out at constant heat flux conditions of $q = 226.9$ kW/m^2, 305.7 kW/m^2, 362.4 kW/m^2, 417.8 kW/m^2, and 497.8 kW/m^2, respectively, with inlet water temperature at 35 °C. It was found that the boiling flow pattern depends greatly on the heat-to-mass flux ratio, q/G, which is related to the Boiling number, Bo, by

$$\mathrm{Bo} = q/Gh_{\mathrm{fg}},$$

where h_{fg} is the latent heat of evaporation.

We now define the "stable flow boiling" mode as under a constant heat flux condition, when the mass flux is constant while temperature and pressure fluctuations are negligibly small or zero. On the other hand, the "unstable flow boiling" mode is defined as under constant heat flux condition, the mass flux keeps on decreasing with time and with appreciable temporal variations of pressure or wall temperatures.

Fig. 4 presents a map showing stable and unstable flow boiling regimes, which is characterized by the two parameters of heat flux q and mass flux G. It is shown that stable flow boiling with no periodic oscillation existed for $q/G < 0.96$ kJ/kg, unstable flow boiling regime with long-period oscillation (more than 1 s) ranged from $q/G = 0.96$ kJ/kg to $q/G = 2.14$ kJ/kg, and unstable flow boiling regime with short-period oscillation (less than 0.1 s) existed for $q/G > 2.14$ kJ/kg in the parallel microchannels for an inlet water temperature of 35 °C.

3.1.1. Stable flow boiling regime with no periodic oscillation ($q/G < 0.96$ kJ/kg)

Fig. 5 shows the four stable boiling flows at $q = 35.4$ kW/m^2 for different values of G near the outlet location. At $G = 55.3$ kg/m^2 s (i.e., $q/G = 0.64$ kJ/kg), isolated bubble grew in the microchannels and then it was flushed downstream by the bulk flow as shown in Fig. 5a. At a small mass flux at $G = 51.3$ kg/m^2 s (i.e., $q/G = 0.69$ kJ/kg), isolated bubble grew and elongated before it was flushed downstream by the bulk flow as shown in Fig. 5b. At a mass flux equal to $G = 48.5$ kg/m^2 s (i.e., $q/G = 0.73$ kJ/kg), bubbles began to coalesce and form a large bubble before it was flushed downstream by the incoming flow as shown in Fig. 5c. Finally, at a smaller mass flux equal to $G = 43.2$ kg/m^2 s (i.e., $q/G = 0.82$ kJ/kg), the bubble began to expand in both upstream and downstream directions as is shown in Fig. 5d. The outlet water temperature for this stable flow boiling mode was about 95 °C (which was several degrees lower than the saturated temperature corresponding to the exit pressure of the microchannels) while the wall temperatures were at superheated conditions.

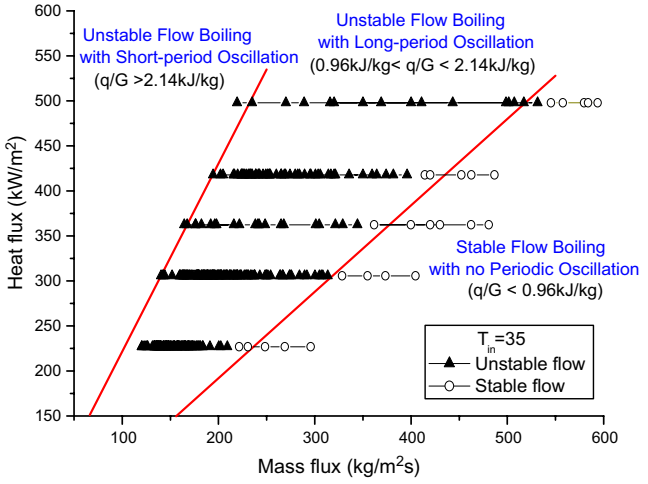

Fig. 4. Stable and unstable flow boiling regimes in parallel microchannels.

3.1.2. Unstable flow boiling regime with long-period oscillation (0.96 kJ/kg $< q/G < 2.14$ kJ/kg)

As mentioned earlier, the mass flux in the unstable flow boiling regime keeps on decreasing under constant heat flux condition. Temporal variations of wall temperatures

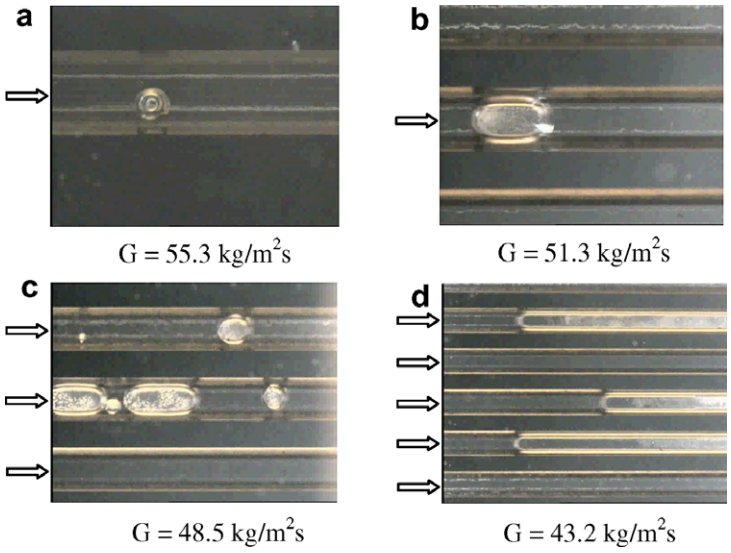

Fig. 5. Photos of flow boiling near the outlet location in stable flow boiling regime ($q/G < 0.96$ kJ/kg) at $q = 35.4$ kW/m^2 and four different G.

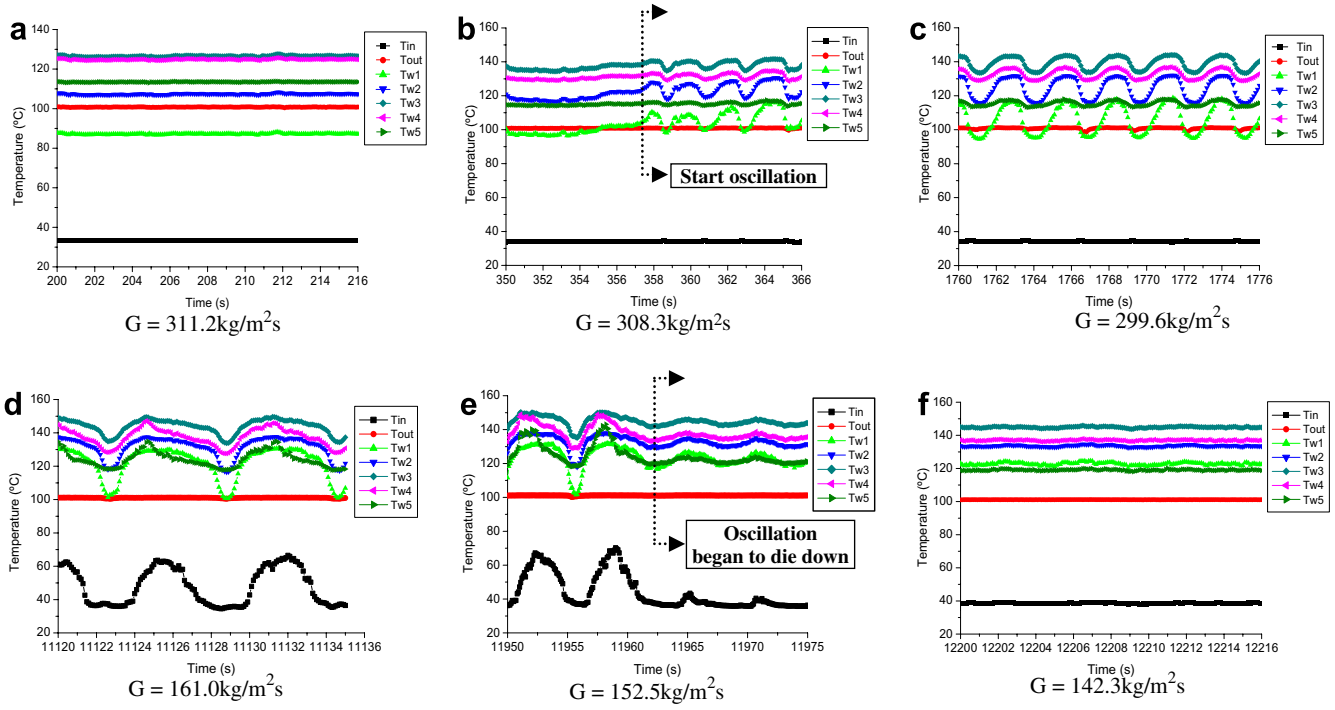

Fig. 6. Oscillation of fluid and wall temperatures in parallel microchannels in the unstable flow regime with long-period oscillation at $q = 305.7$ kW/m^2, and $T_{in} = 35$ °C, as G decreasing from 308.3 to 142.3 kg/m^2 s for the period from $t = 200$ s to $t = 12216$ s.

at $q = 305.7$ kW/m^2 with inlet water temperature at 35 °C as G decreasing from 308.3 to 142.3 kg/m^2 s for the period from $t = 200$ s to $t = 12216$ s are shown in Fig. 6. Just before oscillation started (at $t = 216$ s) with a corresponding mass flux at 311.2 kg/m^2 s, all temperature measurements remained constant with time, which are presented as straight lines shown in Fig. 6a, which corresponded to the stable flow boiling condition. However, about 35 s later, temperature oscillations began to occur as the corresponding mass flux decreased to 308.3 kg/m^2 s as shown in Fig. 6b. A comparison of Fig. 6c (at $G =$ 299.6 kg/m^2 s and at 1760 s $< t <$ 1776 s) and Fig. 6d (at $G = 161.0$ kg/m^2 s and at 11 120 s $< t <$ 11 136 s) shows that cyclic variations of wall temperature periods, oscillation amplitudes, and the average values of temperature increased with the time. The variations of the wall temperature became smaller at $t = 11963$ s. Finally, there were only small variations of temperature beginning at $t = 12200$ s as shown in Fig. 6f (where the corresponding mass flux decreased to 142.3 kg/m^2 s) which corresponded to the unstable flow boiling with short-period oscillation condition. Thus, the long- period of oscillatory flow boiling lasted about 11 843 s (from

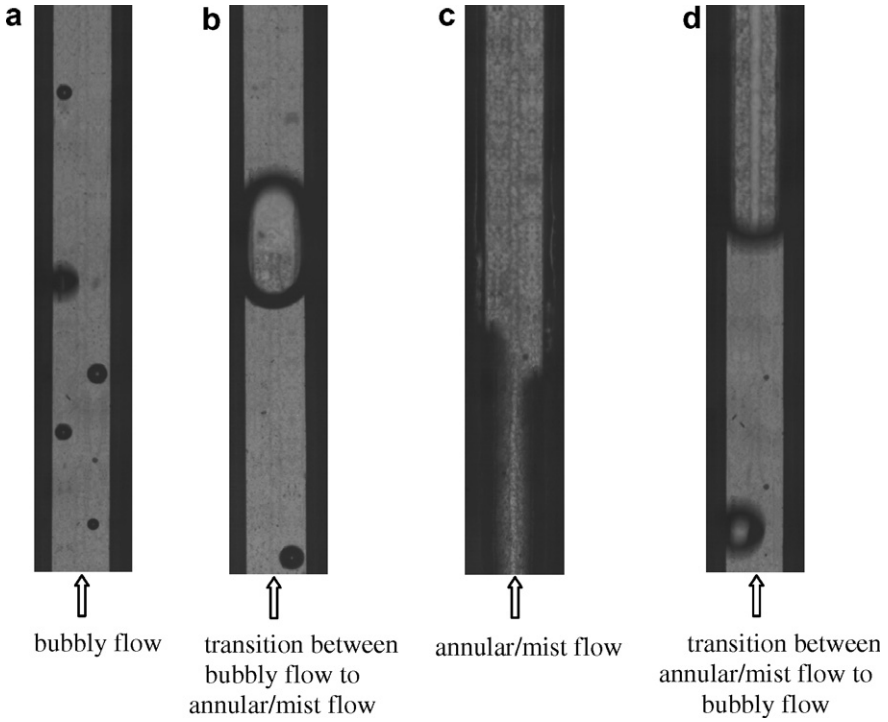

Fig. 7. Photos of alternating flow patterns in one period from (a) to (d) taken at 6325 frame/s in the unstable flow boiling regime with long-period oscillation at $q = 305.7\ \text{kW/m}^2$, $G = 304.7\ \text{kg/m}^2\,\text{s}$ ($q/G = 1.0\ \text{kJ/kg}$), and $T_{\text{in}} = 35\ ^\circ\text{C}$.

starting oscillation at $t = 357$ s to end oscillation at $t = 12\,200$ s).

Figs. 7a–d are the photos for flow patterns during one period at $q = 305.7\ \text{kW/m}^2\,\text{s}$ and at a specific mass flux $G = 304.7\ \text{kg/m}^2\,\text{s}$ (with $q/G = 1.0\ \text{kJ/kg}$) which is in the unstable flow boiling regime shown in Fig. 6b. The photos were taken from the top through the transparent cover with a microscope lens of 50 magnifications at an upstream location (between T_{w1} and T_{w2}) at a frame rate of 6320 frame/s. The bulk flow direction was from bottom to top. It can be seen from Fig. 7a that small bubbles (with a diameter less than 100 μm) were initially formed on the surface of microchannels (having a bottom width of 208 μm). The bubbles were subsequently flushed out of the channels at a speed of 0.60 m/s. At a later time, as shown in Fig. 7b, another bubble at the same location was allowed to grow larger and after it encountered other heated walls or the top pyrex glass cover, it began to expand rapidly in both upstream and downstream directions at a speed of 0.32 m/s and 0.90 m/s, respectively. The reversed flow of vapor increased wall temperatures as well as inlet pressure. The bubble expansion caused transition from bubbly flow to annular/mist flow as shown in Fig. 7c, which had been identified as the main source of instability in the unstable flow boiling regime with long-period oscillation. During the annular flow with a thin annular film along the channel wall, the transient heat conduction and interface evaporation enhanced heat transfer in the channels and reduced the local wall surface temperature. The gradual depletion of the liquid film due to evaporation caused occurrence of mist flow downstream, leading to the intermittent drying (mist flow) and rewetting (annular flow) in the channel wall. Fig. 7d shows the transition from annular/mist flow to bubbly flow. The vapor in the microchannels was observed to be quickly condensed by the incoming flushing liquid, resulting in the decrease in wall temperatures and inlet pressure. Small bubbles followed several long bubbles, and the bubbly flow shown in Fig. 7a occurred again. Generally, alternating flow patterns in the unstable flow boiling regime with long-period oscillation can be described as follows: it began with bubbly flow that subsequently changed to annular/mist flow due to rapid bubble expansion. A new cycle started when the subcooled liquid entered from the inlet and bubbly flow began to occur again.

The cyclic oscillations of temperature of T_{w1} and T_{w2} as well as inlet/outlet pressure during a cycle for the above case of $q = 305.7\ \text{kW/m}^2$ at $G = 304.7\ \text{kg/m}^2\,\text{s}$ ($q/G = 1.0\ \text{kJ/kg}$) are presented in Fig. 8. The oscillation periods of temperature were in agreement with those by the visualization study. This illustrated that the oscillations of temperature were caused by alternating flow patterns. The corresponding flow regions at different times were also indicated in Fig. 8. Note that oscillations of temperature of T_{w1} and T_{w2} (see Fig. 8a) and inlet pressure (see Fig. 8b) were nearly in phase. This confirmed that the occurrence of alternating flow pattern, bubbly flow and annular/mist flow, caused pressure drop fluctuations, which was also reported by Hetsroni et al. [16].

Time-average oscillation amplitudes and average values of all measurements in parallel microchannels in the unstable flow boiling regime with long-period oscillation at

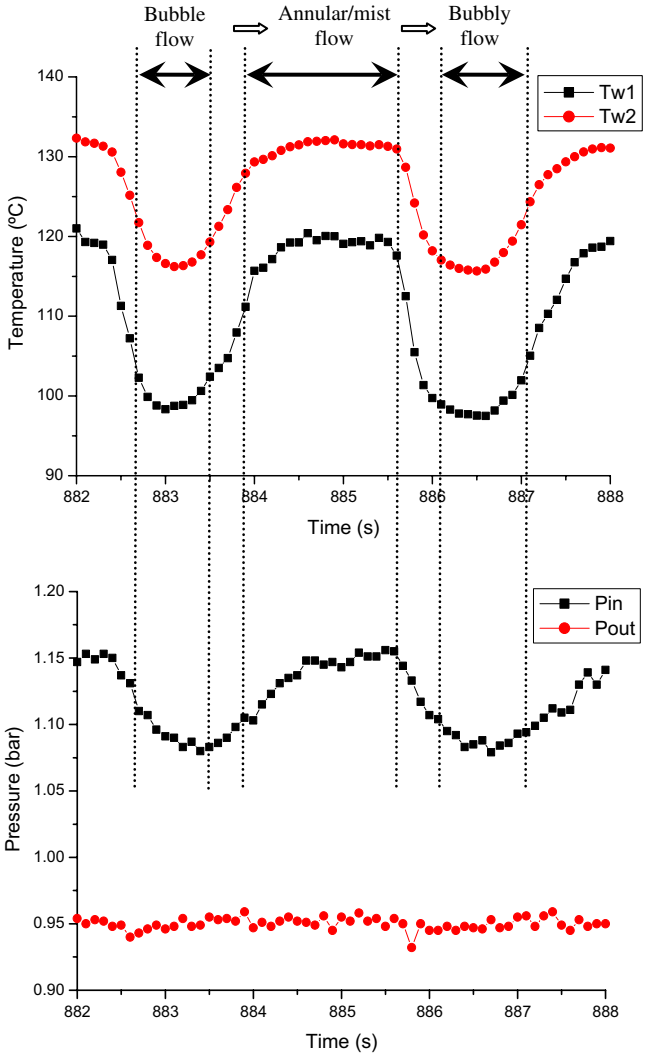

Fig. 8. Oscillations of wall temperatures and inlet/outlet pressure in parallel microchannels in the unstable flow boiling regime with long-period oscillation at $q = 305.7\ \mathrm{kW/m^2}$, $G = 304.7\ \mathrm{kg/m^2\,s}$ ($q/G = 1.0\ \mathrm{kJ/kg}$), and $T_{in} = 35\ ^\circ\mathrm{C}$.

$q = 305.7\ \mathrm{kW/m^2}$ as G decreasing from 311.2 to 142.3 kg/m^2 s (during $t = 2005$ s to $t = 12\,260$ s) are listed in Table 1. The time-average values of these quantities and their oscillation amplitudes were obtained based on a 60 s data acquisition sample. It can be concluded from Table 1 that: (i) the outlet water temperature was almost at the saturation temperature of 100 °C while the average inlet water temperature increased with time, varying from the lowest 33.4 °C to the highest 48.4 °C, and then decreased to a constant value of 38.6 °C. Other time-average measurements including temporal variation of five wall temperatures, as well as inlet pressure increased with time and approached constant values with the former approaching superheated condition; (ii) the highest time-average wall temperature appeared near the middle location (T_{w3}) instead of the outlet location (T_{w5}), which agrees with our previous work [12,13]. However, the highest time-average oscillation amplitude of wall temperatures existed near the inlet location (T_{w1}); and (iii) it is interesting to note that although the mass flux decreased with time and oscillation periods of temperature increased with time as the heat flux remained constant, oscillation period of temperature was dependent only on the heat-to-mass flux ratio, q/G, but independent of the heat flux as shown in Fig. 9. In fact, the oscillation period increased from about 2.5 s to approximately 9.5 s as the value of q/G increased from 0.83 to 2.1 kJ/kg.

3.1.3. Unstable flow boiling regime with short-period oscillation ($q/G > 2.14$ kJ/kg)

Unstable flow boiling regime existed also for the case of $q/G > 2.14$ kJ/kg, where short-period/small-amplitude pressure oscillation existed although temperature oscillations were small. For the case of $q = 305.7\ \mathrm{kW/m^2}$ and $G = 65.2\ \mathrm{kg/m^2\,s}$ ($q/G = 4.69$ kJ/kg), Fig. 10a shows that variations of inlet/outlet water temperatures and outlet pressure were almost constant while the oscillation frequency of inlet pressure was at 22 Hz. It is of interest to note that periodic noises could be heard during this mode of flow boiling. For this type of unstable boiling flow, the backward expansion of the vapor bubble had entered deep into the inlet plenum, causing strong mixing with incoming subcooled water. Because of the relatively cold water in the inlet plenum, strong condensation took place at the vapor–liquid interface that caused sharp shrinking of the vapor plug, resulting in the occurrence of inlet pressure oscillation and noise. The highest pressure during one cycle was considered to be generated at the collapse of the vapor plug and to be a kind of cavitations [18,19]. The frequency of pressure fluctuations corresponded to the number of noise generated per second.

Fig. 10b shows the variations of temperature and pressure at $q = 305.7\ \mathrm{kW/m^2}$, the same as in Fig. 10a but at a lower mass flux of 38.6 kg/m^2 s ($q/G = 7.92$ kJ/kg). A comparison of the values of temperature and pressure between Figs. 10a and b reveal that (i) the inlet temperature increased with the decrease in mass flux. Because of the vapor bubble expanded in upstream and penetrated into the inlet plenum, causing the water temperature in the plenum T_{in}, higher than that of the incoming subcooled water; (ii) although oscillation amplitudes of inlet pressure increased as the mass flux decreased from 65.2 to 38.6 kg/m^{2}s, the inlet pressure oscillation frequency remained at 22 Hz. Therefore, the frequency of pressure fluctuations was independent of the mass flux. (iii) The inlet and outlet temperatures of water as well as wall temperatures were not oscillatory but nearly constant, which are presented as straight lines. The reason can be explained as follows: the type-T thermocouples used for wall temperatures and inlet/outlet water temperatures had a response time of 0.1 s, which was much longer than the pressure oscillation period of 0.045 s. Thus, it was impossible to measure the temperature oscillation at such a high frequency by these thermocouples.

Table 1
Various quantities in parallel microchannels at $q = 305.7$ kW/m^2 as G decreasing with time from 311.2 to 142.3 kg/m^2 s

Time			T_{in} (°C)	T_{out} (°C)	T_{w1} (°C)	T_{w2} (°C)	T_{w3} (°C)	T_{w4} (°C)	T_{w5} (°C)	P_{in} (bar)	P_{out} (bar)	Mass flux (kg/m^2 s)	Period (s)
From (s)	To (s)												
200	260	Average value	33.4	100.8	87.2	107.4	126.5	124.8	113.5	1.076	0.955	311.2	0
		Oscillation amplitude	0.1	0.5	1.4	1.4	1.6	1.3	0.7	0.015	0.021		
1390	1450	Average value	33.5	98.7	103.2	120.9	136	129.5	112.6	1.09	0.93	302.3	3.32
		Oscillation amplitude	0.9	2.7	23.1	16.7	10.7	8.2	5.2	0.083	0.04		
2580	2640	Average value	33.4	98.2	106.9	121.8	136.2	129.2	115.1	1.096	0.926	290.7	3.54
		Oscillation amplitude	1.3	2.6	27	17.8	11.9	10.4	7.5	0.104	0.044		
3770	3830	Average value	33.7	98.7	106.9	122.8	136.1	129.7	114.4	1.095	0.928	271.6	3.79
		Oscillation amplitude	1.4	5.1	34	22.9	15.8	13.2	8.4	0.114	0.036		
4960	5020	Average value	36.4	97.6	112.3	123.7	136.9	130.2	117.2	1.103	0.921	254.7	4.01
		Oscillation amplitude	14.2	6.2	33.9	24.2	16.9	17.3	12.6	0.13	0.03		
6150	6210	Average value	39.9	99.5	113.8	125.5	137.4	131.5	118.9	1.114	0.938	240.7	4.33
		Oscillation amplitude	21	3.9	35.1	22	16.2	16.5	13.8	0.134	0.05		
7340	7400	Average value	41.3	97.7	113.9	125.5	138.1	131.7	118.3	1.111	0.922	209.38	4.6
		Oscillation amplitude	23.4	5.6	36.9	23.7	17.7	19.8	18.4	0.159	0.036		
8530	8590	Average value	42.3	98.5	115.1	125.7	137.3	131.5	119	1.119	0.926	203.8	4.76
		Oscillation amplitude	25.1	2.8	33.6	22.1	17.7	20.6	21.1	0.137	0.024		
9720	9780	Average value	43.8	99.3	116.6	127.5	140.2	133.8	120.6	1.128	0.936	191.0	5.57
		Oscillation amplitude	30.9	6	34.7	24.3	17.4	18.8	17	0.151	0.047		
10910	10970	Average value	48.4	97.5	118.9	127.4	139.5	133.7	121.1	1.129	0.916	175.3	6.59
		Oscillation amplitude	33.5	2.9	36.6	25.9	17.8	22.4	24.9	0.157	0.025		
12200	12260	Average value	38.6	99.5	120.5	131.3	142.4	134.8	119.1	1.139	0.935	142.3	0
		Oscillation amplitude	1.7	0.1	4.7	2.2	1.9	1.9	2.1	0.028	0.018		

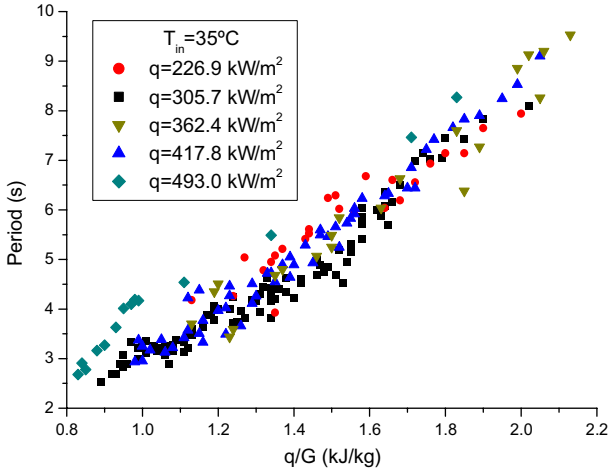

Fig. 9. Oscillation periods of temperature vs. heat-to-mass flux ratio at different heat flux in parallel microchannels in the unstable flow boiling regime with long-period oscillation.

Figs. 11a and b show the variations of temperature and pressure at a higher heat flux at 740.7 kW/m^2 at two mass fluxes of 162.2 ($q/G = 4.57$ kJ/kg) and 136.6 kg/m^2 s ($q/G = 5.42$ kJ/kg) in the unstable flow boiling regime with short-period oscillation. As shown from these figures, the oscillation frequency of inlet pressure for both cases was about 32 Hz. By comparing the frequency at different heat fluxes shown in Figs. 10 and 11, the frequency of inlet pressure oscillation in this type of unstable flow boiling regime increased with the increase in heat flux, but was independent of the mass flux.

Figs. 12a and b are the photos for flow pattern in two neighboring microchannels during one cycle taken at a frame rate of 5000 frame/s at $q = 305.7$ kW/m^2 and $G = 65.2$ kg/m^2 s ($q/G = 4.69$ kJ/kg) corresponding to the case shown in Fig. 10a. Fig. 12a shows that mist/superheated flow was followed by the annular flow in Fig. 12b. About half of period, 0.0227 s, was occupied by one of these two alternating flow patterns, which are also indicated in Fig. 10a. It is interesting to note that the transition between mist/superheated and annular flow in all parallel microchannels occurred synchronously.

3.2. Flow boiling patterns in a single microchannel

Experiments were also performed for flow boiling in a single microchannel heated at constant heat fluxes of $q = 84.5$ kW/m^2, 157.0 kW/m^2, 222.3 kW/m^2 and 297.8 kW/m^2,

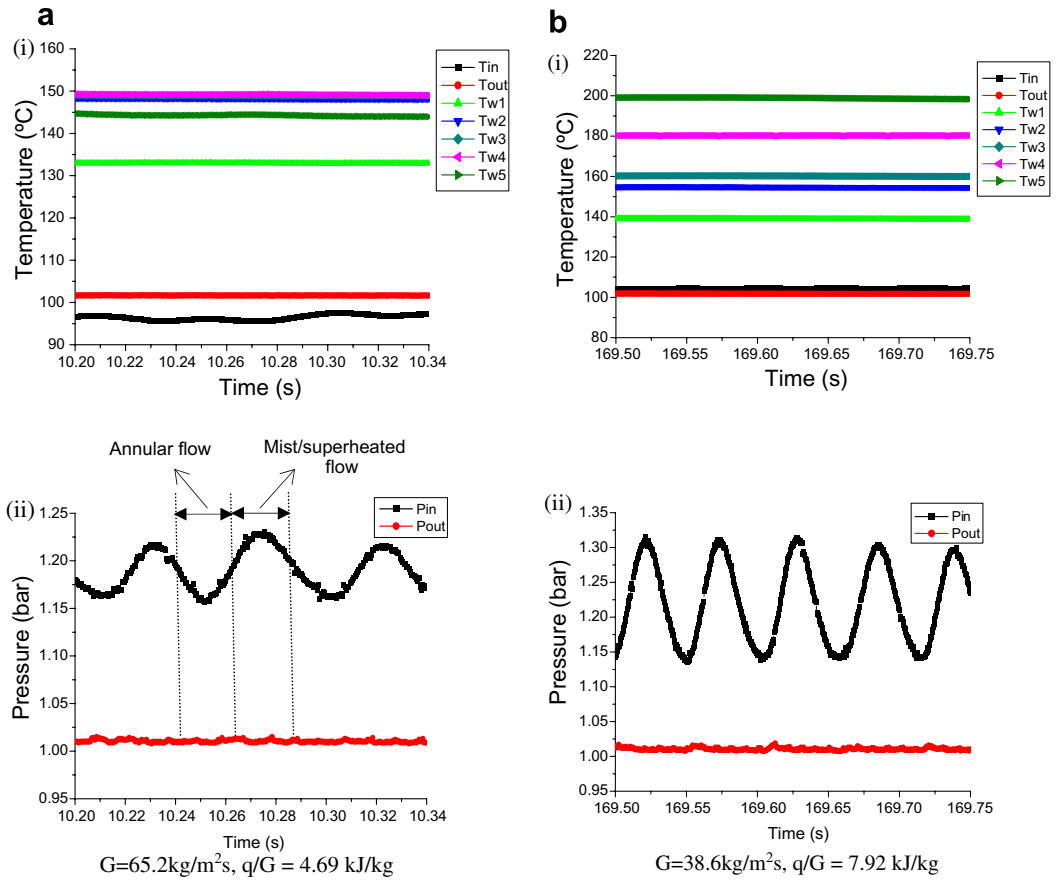

Fig. 10. Measurements of inlet/outlet water and wall temperatures and inlet/outlet pressure in parallel microchannels in the unstable flow boiling regime with short-period oscillation at $q = 305.7$ kW/m^2, $T_{in} = 35$ °C.

where the last two heat fluxes were approximately the same as those in parallel microchannels (as discussed in Section 3.1) for comparison purpose. Fig. 13 presents the flow pattern map in terms of heat flux versus mass flux showing the stable and unstable flow boiling regimes in a single microchannel. It is shown that stable flow boiling regime with no periodic oscillation and unstable flow boiling regime with short-period oscillation (less than 0.1 s) occurred for $q/G < 0.09$ kJ/kg and $q/G > 0.32$ kJ/kg, respectively, and unstable flow boiling regime with long-period oscillation (more than 10 s) existed for 0.09 kJ/kg $< q/G <$ 0.32 kJ/kg. A comparison of Figs. 4 and 13 shows that the unstable flow boiling regime with long-period oscillation in a single microchannel is smaller than that in parallel microchannels. This implies that flow interaction from neighboring channels promotes instability in the microchannel. Since the stable boiling flow in a single microchannel is similar to those in parallel microchannels, we will discuss only the cases of unstable flow boiling with long-period and short-period oscillations in the following paragraphs.

3.2.1. Unstable flow boiling regime with long-period oscillation (0.09 kJ/kg < q/G < 0.32 kJ/kg)

Reversed flow of vapor had been found in flow boiling phenomenon in parallel minichannels and microchannels [11,15,17]. The presence of the parallel channels was conducive to the occurrence of reversed flow, which allowed a path of lower flow resistance. The flow and pressure in the other channels compensated the high-pressure due to vapor generation to dissipate through the other channels. A reversed flow and local dry-out condition were also observed previously in flow boiling in a single microchannel [10].

Fig. 14 shows the changing flow boiling patterns in a single microchannel at $q = 84.5$ kW/m^2 and $G = 453.9$ kg/m^2 s ($q/G =$ 0.186 kJ/kg) which was in the unstable flow boiling regime with long-period oscillation. The photos were taken at 6640 frame/s, which gave the progression of reversed flow. Figs. 14a and b show that a bubble nucleated in the channel initially at $t = 0$. Figs. 14c and d show that the bottom side of the liquid–vapor interface moved toward the channel entrance from $t = 2.56$ ms to 3.31 ms, counter to the flow direction which was from bottom to top. The life time of the vapor core expansion, from Fig. 14c and d, was about 0.75 ms, which agrees with those obtained by Hetsroni et al. [16], who concluded that at the specified conditions of the experiment, the life time of the elongated bubble did not exceed 0.001 s. Fig. 14e shows that the channel wall began at dry-out condition at $t =$ 19.4 ms because of the rapid evaporation of the liquid film in the microchannel. The life time of the local dry-out con-

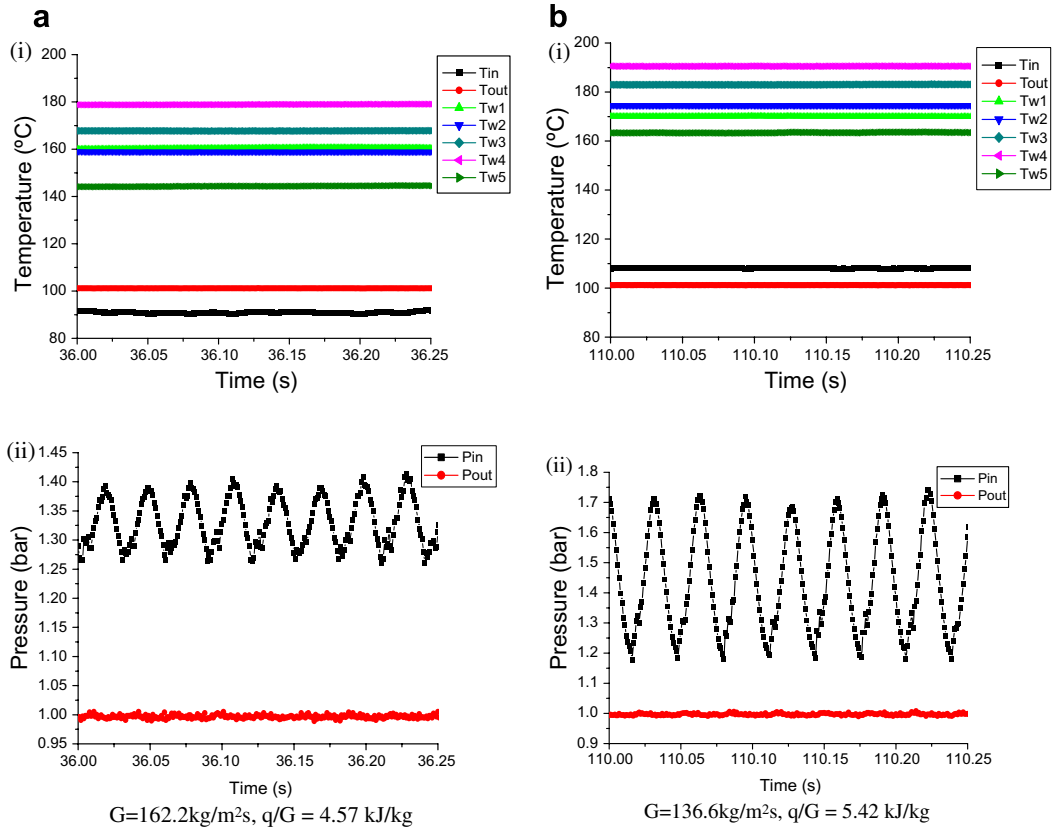

Fig. 11. Measurements of inlet/outlet water and wall temperatures and inlet/outlet pressure in parallel microchannels in the unstable flow boiling regime with short-period oscillation at $q = 740.7\ \text{kW/m}^2$, $T_{in} = 35\ ^\circ\text{C}$.

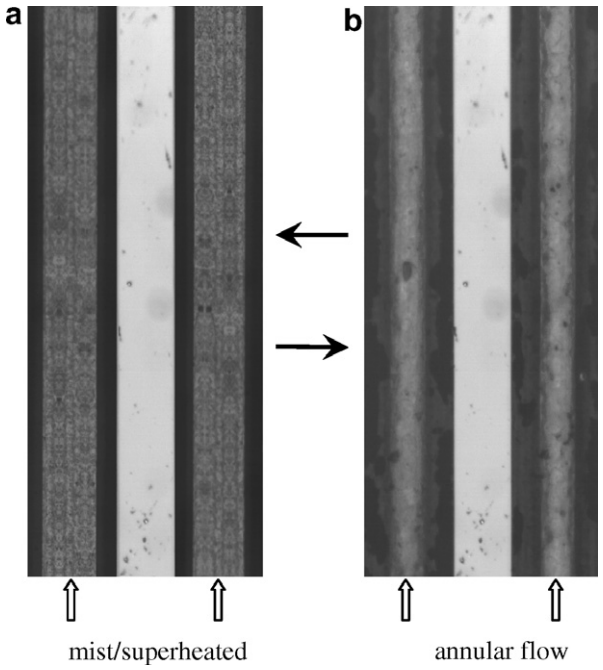

Fig. 12. Photos of the unstable flow boiling patterns with short-period oscillation in one cycle from (a) to (b) in parallel microchannels at $q = 305.7\ \text{kW/m}^2$, $G = 65.2\ \text{kg/m}^2\,\text{s}$, and $T_{in} = 35\ ^\circ\text{C}$. Photos were taken at 5000 frame/s.

dition was about 18.98 ms, which was much longer than that of the vapor core expansion of 0.75 ms. As shown in

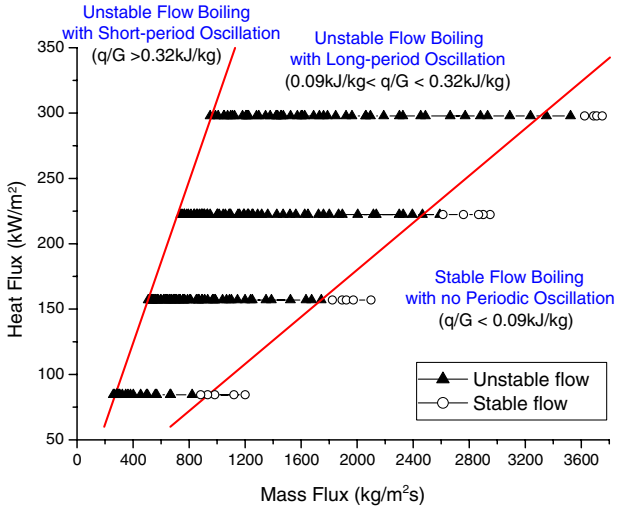

Fig. 13. Stable and unstable flow boiling regimes in a single microchannel.

Fig. 14f and h, the bottom side of the liquid–vapor interface moved toward the channel exit from $t = 22.7$ ms to 23.9 ms during the annular flow.

The flow pattern transition instability in a single microchannel was similar to that in parallel microchannels as discussed in the preceding paragraphs. The trigger mechanism of such instability was venting vapor core due to very rapid expansion. Fig. 15 shows temporal temperature oscillations

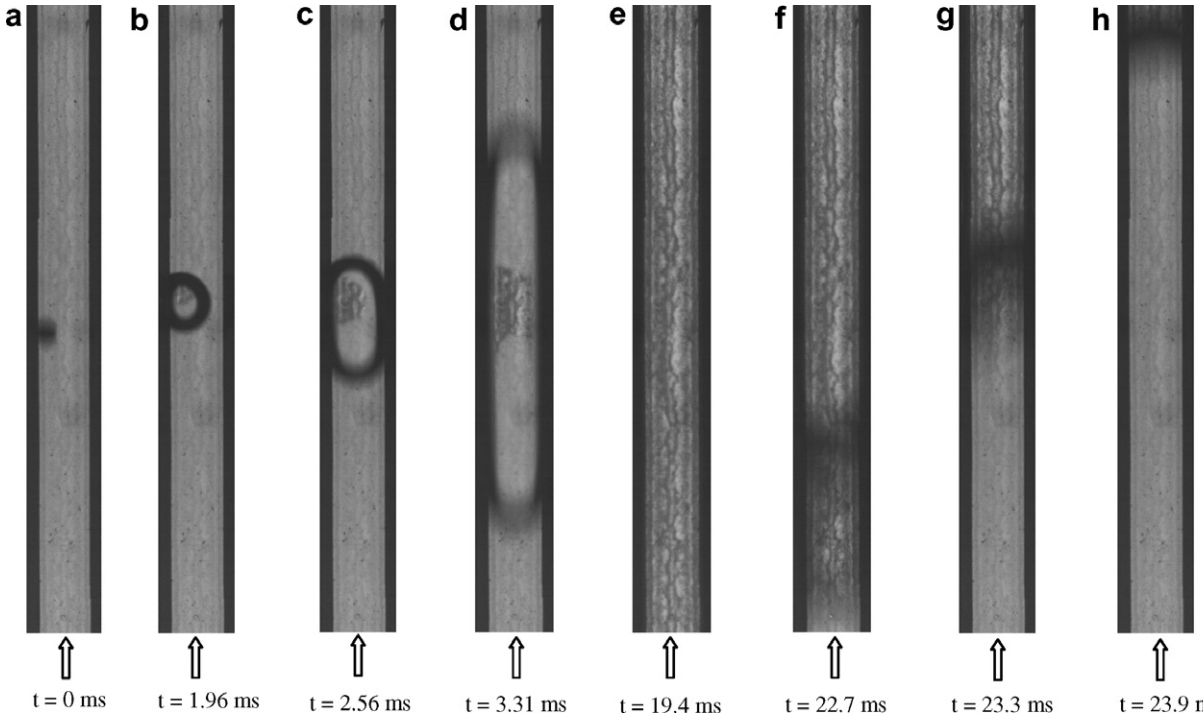

Fig. 14. Photos of flow patterns during the unstable flow boiling regime with long-period oscillation in a single microchannel at $q = 84.5\ \mathrm{kW/m^2}$, $G = 453.9\ \mathrm{kg/m^2\,s}$, and $T_{in} = 35\ ^\circ\mathrm{C}$. Photos were taken at 6640 frame/s.

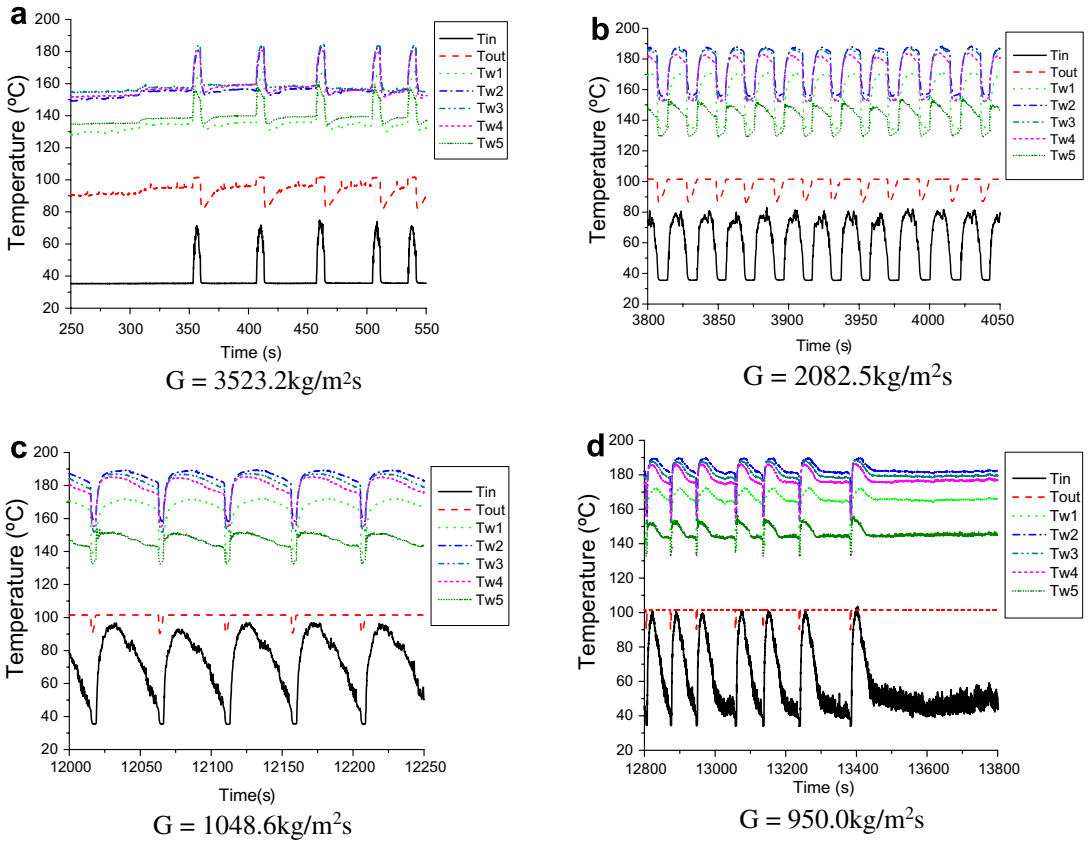

Fig. 15. Oscillation of fluid and wall temperatures in a single microchannel in the unstable flow boiling regime with long-period oscillation at $q = 297.8\ \mathrm{kW/m^2}$ and $T_{in} = 35\ ^\circ\mathrm{C}$, as G decreasing with time from 3523.2 to 950.0 $\mathrm{kg/m^2\,s}$.

at $q = 297.8$ kW/m^2 with inlet water temperature at 35 °C. A comparison of Figs. 6 and 15 reveal that due to the lack of flow interaction from other channels, the corresponding mass fluxes and oscillation periods of temperature in single microchannel were larger than those in parallel microchannels. For example, the mass flux in a single microchannel for $q = 297.8$ kW/m^2 varied from 3523.2 kg/m^2 s at the beginning of the cycle to 950.0 kg/m^2 s at the end of the cycle as compared that from 308.3 to 142.3 kg/m^2 s for $q = 305.7$ kW/m^2 in parallel microchannels. When the unstable flow boiling with long-period of oscillation changed to short-period oscillation as the mass flux decreased to 950.0 kg/m^2 s in the single microchannel and 142.3 kg/m^2 s in the parallel microchannels, the inlet temperature in a single microchannel was about 45.9 °C, which was larger than that in parallel microchannels, 38.6 °C. The range of the wall temperatures in a single microchannel was from 145 °C (T_{w5}) to 182 °C (T_{w2}) as shown in Fig. 6f while that in parallel microchannels was from 119 °C (T_{w5}) to 145 °C (T_{w3}) as shown in Fig. 15d.

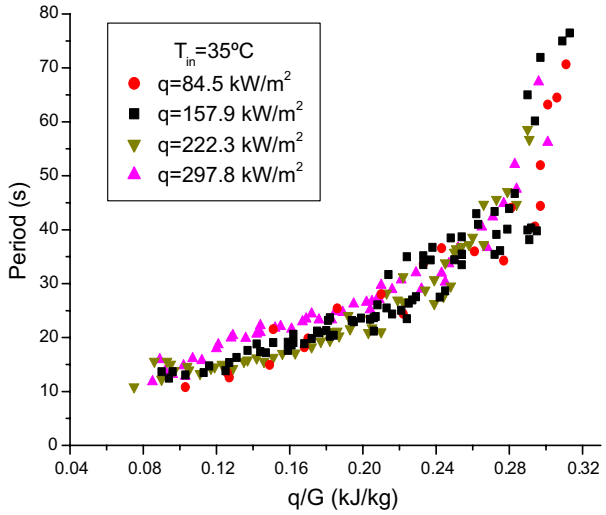

Fig. 16. Oscillation periods of temperature vs. heat-to-mass flux ratio at different heat fluxes in a single microchannel in the unstable flow boiling regime with long-period oscillation.

Fig. 16 shows that oscillation periods of temperature increased from 10 to 80 s in the unstable flow boiling regime when the heat-to-mass flux ratio, q/G, increased from 0.09 to 0.32 kJ/kg at different heat fluxes in a single microchannel. It can be seen that oscillation periods of

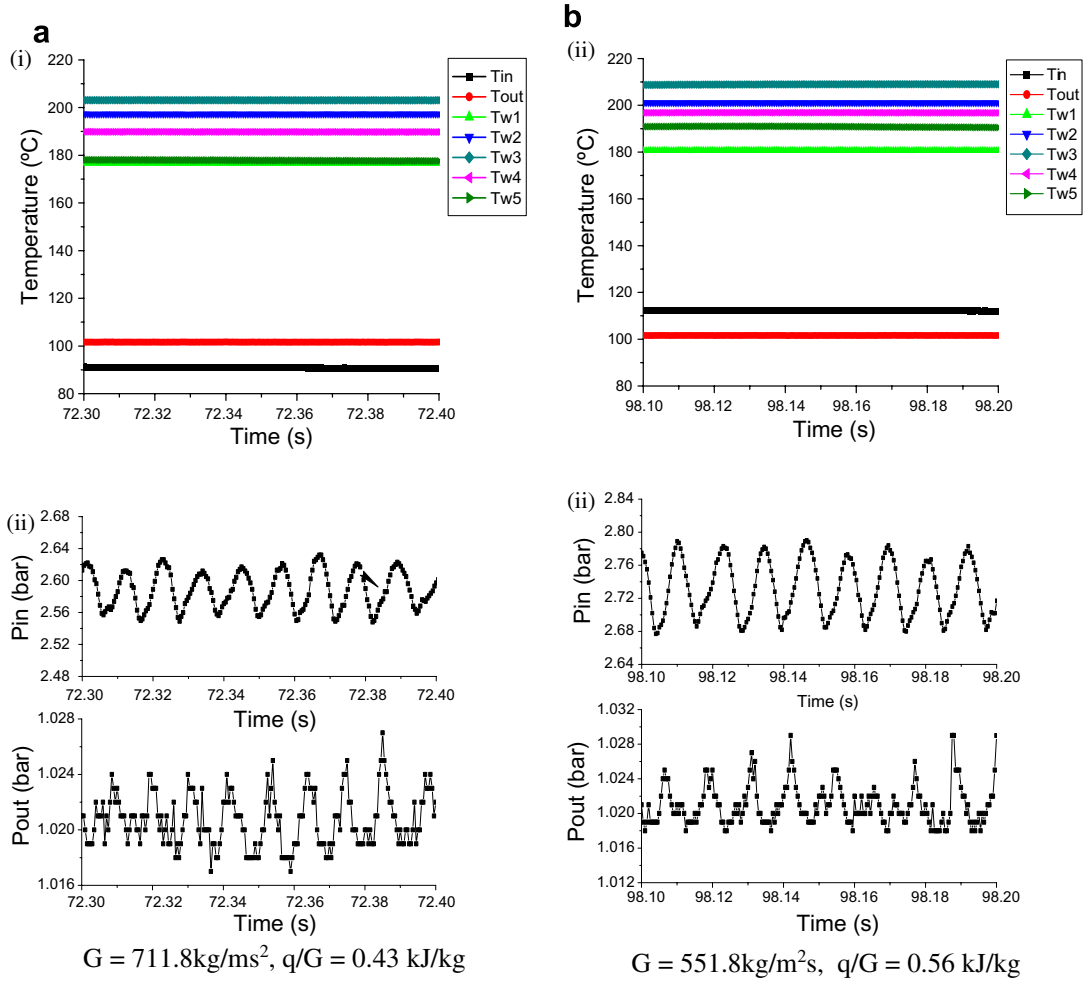

Fig. 17. Measurements of inlet/outlet water and wall temperatures and inlet/outlet pressure in a single microchannel in the unstable flow boiling regime with short-period oscillation at $q = 307.6$ kW/m^2, $T_{in} = 35$ °C.

temperature depended only on the heat-to-mass flux ratio, but independent of the heat flux, which was the same as that in parallel channels. However, by comparing Fig. 9 with Fig. 16, the oscillation periods of temperature in single channel (varying from 10 to 80 s) were much longer than those in parallel channels (varying from 2.5 to 9.8 s). Also, the relationship of oscillation periods of temperature versus the heat-to-mass flux ratio in a single microchannel was parabolic while that in parallel microchannels was linear.

3.2.2. *Unstable flow boiling regime with short-period oscillation (q/G > 0.32 kJ/kg)*

Fig. 17 shows the oscillations of temperature and pressure in this type of unstable flow boiling regime for $q = 307.6\ \mathrm{kW/m^2}$ at two constant mass fluxes of $G = 711.82$ ($q/G = 0.43$ kJ/kg), and 551.8 kg/m^2 s ($q/G = 0.56$ kJ/kg), respectively. The oscillation frequency of inlet pressure for both cases was about 90 Hz, which was larger than that in parallel microchannels at 22 Hz. The inlet and outlet pressures were out of phase in this case while there was no distinct oscillation of outlet pressure in parallel microchannels (see Figs. 10b and 11b). The oscillation of outlet pressure was probably caused by higher mass fluxes (711.8 and 551.8 kg/m^2 s) than those in parallel microchannels (65.2 and 38.6 kg/m^2 s).

Fig. 18 shows the oscillations of temperature and pressure at a higher heat flux, $q = 495.4\ \mathrm{kW/m^2}$ at two constant mass fluxes of $G = 895.2$ ($q/G = 0.55$ kJ/kg), and 679.5 kg/m^2 s ($q/G = 0.73$ kJ/kg) in the unstable flow boiling regime with short-period oscillation. The oscillation frequency of inlet pressure for both cases was about 156 Hz. A comparison of Figs. 17 and 18 reveals that the oscillation amplitudes and frequency of inlet pressure increased with the increase in heat flux, but the frequency was independent of the mass flux, which was similar with those in parallel microchannels.

4. Concluding remarks

In this paper, simultaneous visualization and measurements of temperature, pressure and mass flux variations have been carried out to investigate flow boiling instabilities of water in parallel microchannels and a single microchannel, both having a hydraulic diameter of 186 μm with inlet water temperature at 35 °C. Flow pattern transition instabilities in both parallel microchannels and a single microchannel were observed. The alternating flow patterns were observed by a high-speed video recording system, and the oscillations of temperature as well as inlet/outlet pressure were recorded. The following conclusions can be drawn:

1. There are three flow boiling modes in parallel microchannels and in a single microchannel, depending on

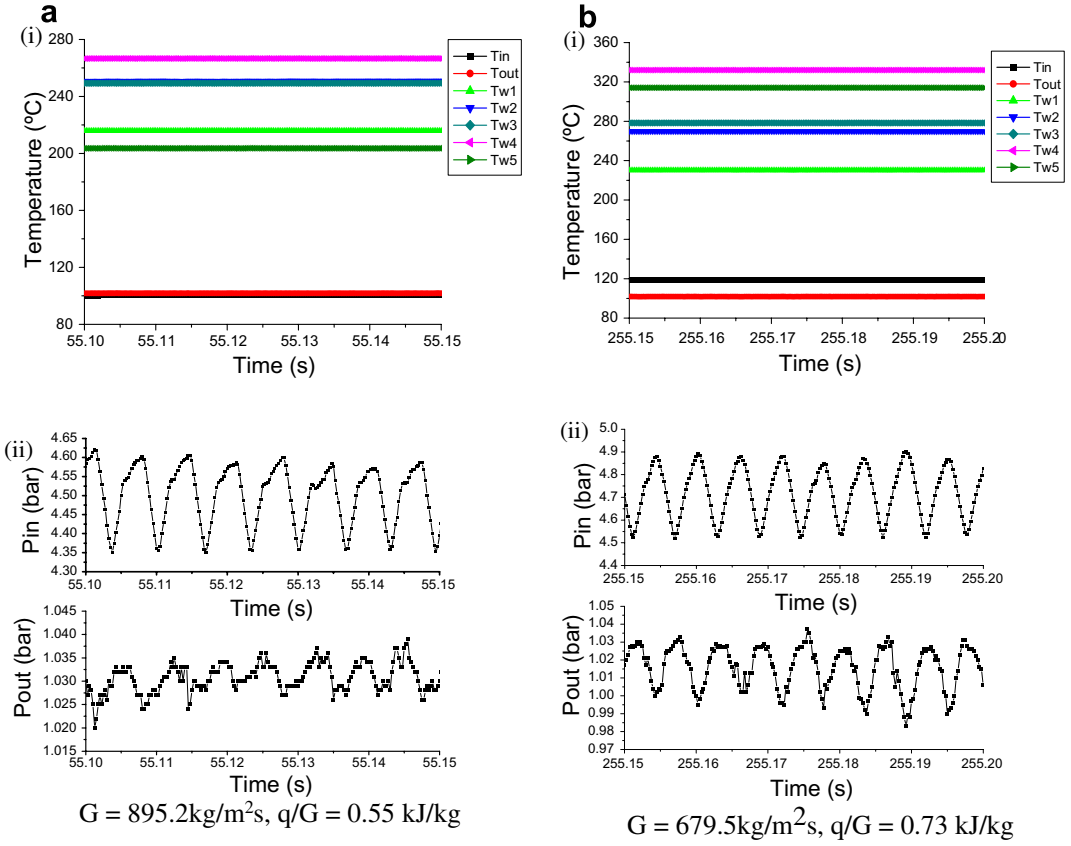

Fig. 18. Measurements of inlet/outlet water and wall temperatures and inlet/outlet pressure in a single microchannel in the unstable flow boiling regime with short-period oscillation at $q = 495.4\ \mathrm{kW/m^2}$, $T_{in} = 35$ °C.

the heat-to-mass flux ratio, q/G. These are: (i) stable boiling flow regime with no periodic oscillation; (ii) unstable flow boiling regime with long-period oscillation (more than 1 s) and (iii) unstable flow boiling regime with short-period oscillation (less than 0.1 s).

2. Stable flow boiling existed for $q/G < 0.09$ kJ/kg and $q/G < 0.96$ kJ/kg in single microchannel and in parallel microchannels, respectively. In this stable flow boiling mode, isolated bubbles grew, elongated and then were flushed downstream by the bulk flow.
3. Unstable flow boiling with long-period oscillation mode existed for $0.96\ \text{kJ/kg} < q/G < 2.14\ \text{kJ/kg}$ in parallel microchannels, and for $0.09\ \text{kJ/kg} < q/G < 0.32\ \text{kJ/kg}$ in a single microchannel. This instability is owing to the periodic bubble expansion in both upstream and downstream directions, causing the increase in wall temperature and inlet pressure. This type of instability is unique in microchannels owing to the confined space of the microchannels. Although the mass flux decreases and oscillation period of temperature varies with time in the unstable flow boiling regime, oscillation period of temperature is dependent on the heat-to-mass flux ratio, q/G, but independent of the heat flux. The oscillation periods of temperature in a single channel (varying from 10 to 80 s) are much longer than those in parallel channels (varying from 2.5 to 9.8 s) with the same hydraulic diameter and at the same heat flux condition.
4. Unstable flows boiling with short-period oscillation existed when the vapor bubble expands periodically upstream into the plenum and in direct contact with the incoming subcooled liquid. The oscillation magnitude of inlet pressure fluctuations increases with the increase in heat flux in both parallel channels and a single channel. The inlet pressure oscillation is higher in a single channel than that in parallel channels. Periodic noises could be heard and the frequency (i.e., the number of the noise per second) was found in agreement with that of inlet pressure fluctuations and from the visualization study. These noises have never been reported in the literature on flow boiling in microchannels.

Acknowledgements

This work was supported by the National Natural Science Foundation of China through Grant No. 50536010 and by Shanghai Municipal Science and Technology Committee through Grant No. 05JC14025. The authors would also like to thank Prof. A. E. Bergles of R. P. I. for helpful discussion and his critical reading of the manuscript.

References

[1] J.A. Boure, A.E. Bergles, L.S. Tong, Review of two-phase flow instability, Nucl. Eng. Des. 25 (1973) 165–192.
[2] H. Yuncu, O.T. Yildirim, S. Kakac, Two-phase flow instabilities in a horizontal single boiling channel, Appl. Sci. Res. 48 (1991) 83–104.
[3] Y. Ding, S. Kakac, X.J. Chen, Dynamic instability of boiling two-phase flow in a single horizontal channel, Exp. Therm. Fluid Sci. 11 (1995) 327–342.
[4] Q. Wang, X.J. Chen, S. Kakac, Y. Ding, Boiling onset oscillation: a new type of dynamic instability in a forced-convection upflow boiling system, Int. J. Heat Fluid Flow 17 (4) (1996) 418–423.
[5] A.E. Bergles, Burnout in boiling heat transfer. Part O: high-quality forced-convection systems, Accident Anal. 20 (1979) 671–689.
[6] R.S. Thurston, J.D. Rogers, V.J. Skoglund, Pressure oscillation induced by forced convection heated in dense hydrogen, Adv. Cryogenic Eng. 12 (1967) 438–447.
[7] J.L. Xu, S. Shen, Y.H. Gan, Y.X. Li, W. Zhang, Q.C. Su, Transient flow pattern based microscale boiling heat transfer mechanisms, J. Micromech. Microeng. 15 (2005) 1344–1361.
[8] G. Hetsroni, A. Mosyak, Z. Segal, G. Ziskind, A uniform temperature heat sink for cooling of electronic devices, Int. J. Heat Mass Transfer 45 (2002) 3275–3286.
[9] G. Hetsroni, A. Mosyak, Z. Segal, Nonuniform temperature distribution in electronic devices cooled by flow in parallel microchannels, IEEE Trans. Compon. Pack. Technol. 24 (2001) 17–23.
[10] D. Brutin, F. Topin, L. Tadrist, Experimental study of unsteady convective boiling in heated minichannels, Int. J. Heat Mass Transfer 46 (2003) 2957–2965.
[11] W.L. Qu, I. Mudarwar, Measurement and prediction of pressure drop in two-phase micro-channel heat sinks, Int. J. Heat Mass Transfer 46 (2003) 2737–2753.
[12] H.Y. Wu, P. Cheng, Visualization and measurements of periodic boiling in silicon microchannels, Int. J. Heat Mass Transfer 46 (2003) 2603–2614.
[13] H.Y. Wu, P. Cheng, Boiling instability in parallel silicon microchannels at different heat flux, Int. J. Heat Mass Transfer 47 (2004) 3631–3641.
[14] J.L. Xu, J.J. Zhou, Y.H. Gan, Static and dynamic flow instability of a parallel microchannel heat sink at high heat flux, Energ. Convers. Manage. 46 (2005) 313–334.
[15] M.E. Steinke, S.G. Kandlikar, An experimental investigation of flow boiling characteristics of water in parallel microchannels, ASME J. Heat Transfer 126 (2004) 518–526.
[16] G. Hetsroni, A. Mosyak, E. Pogrebnyak, Z. Segal, Explosive boiling of water in parallel micro-channels, Int. J. Multiphas. Flow 31 (2005) 371–392.
[17] S.G. Kandlikar, P. Balasubramanian, An Experimental study on the effect of gravitational orientation on flow boiling of water in 1054×197 μm parallel minichannels, Int. J. Heat Transfer 127 (2005) 820–829.
[18] R.E.A. Arndt, Cavitation in fluid machinery and hydraulic structures, Ann. Rev. Fluid Mech. 13 (1981) 273–328.
[19] C.E. Brennen, S.L. Ceccio, Recent observations on cavitation and cavitation noise, in: Proc. Third Int. Symp. On Cavitation Noise and Erosion in Fluid Systems, San Francisco CA, December 1989, pp. 67–78.